

## Pattern Classification in Subject's Stress State Identification

D.M. Dobra<sup>\*</sup>, H.N. Teodorescu<sup>\*,\*\*</sup>

<sup>\*</sup>Faculty of Electronics and Telecommunication, "Gh. Asachi" Technical University of Iasi,

<sup>\*\*</sup>Romanian Academy

**Abstract:** We demonstrate the ability of the system based on a new multimodal Virtual Joystick interface to recognize the fatigue state for a person who is carrying out activity by using this device like an input one. In this way we develop a method to recognize the fatigue state and to enable a digital computer to sense the user's state. To pursue this goal several methods of signal processing, feature extractor and pattern recognition algorithms are used. Moreover, a methodology used to identify the fatigue state was developed. The Virtual Joystick device is able to sense and track the 3D-hand movement without any physical contact and, simultaneously, to acquire a reliable hand tremor signal. The Virtual Joystick can replace a standard joystick and, more than that, when it receives a request, it has the ability to send, through PC serial line, the continuously acquired tremor signal.

### 1. Introduction

Building high performance interactive computer systems and other "intelligent" systems requires the understanding of both the physical, psychological, emotional user's state and the mode in which a user interacts with such systems. Moreover, the human efficiency in the activity related to the human-computer interaction (or, more general, human-machine interaction) are directly dependent on both, the subject's state and the capability of the systems to recognize the specific needs of the user and to change their response accordingly. Unfortunately, acquiring and interpreting this kind of information is very difficult and, in consequence, the present day systems have only a limited ability of communication. Current strategies for user's state acquisition are either obtrusive (only a few of them are not) or, the data, captured by the systems, consist in a raw information (keystrokes, mouse and standard joystick movements).

Physiological variables have been traditionally used to measure the changes in physical, psychological and emotional state. Typically, biological signals like: heart rate [1], [2], blood pressure [2], [3], galvanic skin response (GSR) [1], [2], [3], temperature [1], [2], [4], respiration [2], [3], [4], somatic movement, as well as electromyography (EMG) [3], electrocardiography (ECG) and electroencephalography (EEG) are used for this purpose.

In our study we use the tremor signal to identify the fatigue state; the signal is acquired with a Virtual Joystick. The Virtual Joystick system developed by us includes the sensor [5], [6], the electronic control unit [7], [8], the software used to interface with the device (used to present the hand position in the input 3D space and to transfer, save and show the tremor signal) [8], and the module used to

compensate the hand variability and to filter the noise introduced by the joystick port acquisition system [9].

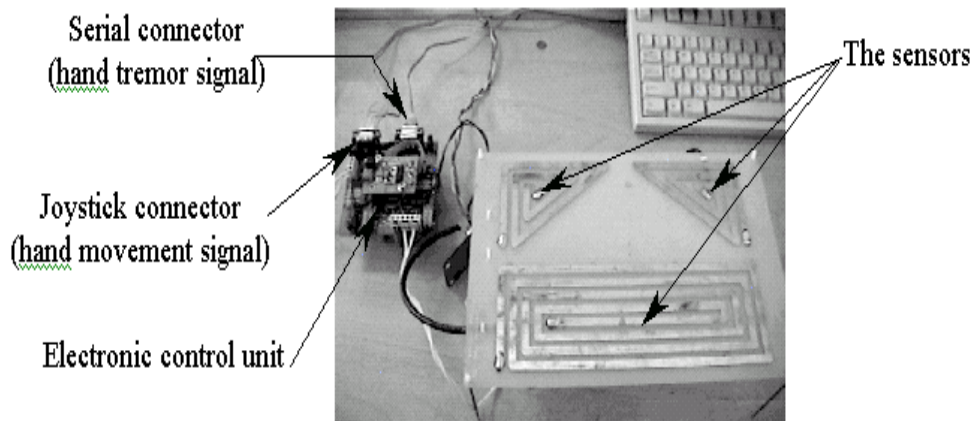


Fig. 1 – The three sensors and the electronic processing system – the Virtual Joystick

The Virtual Joystick has three transducers to perform the hand tracking procedure. In Fig. 1, we show a picture with the practical implementation of the system. The operating principle of the transducers [5], that are part of the Virtual Joystick, is based on the property that an element generating an external electromagnetic field changes its impedance due to the properties of the objects in its close vicinity. When the hand is above one of the sensors, the output of the corresponding circuit has a high value.

The sensors that sense left-right balance are placed symmetrically on the board and are paired, such that the signal from a couple of opposite sensors evidences the balance movements of the hand. The principle is similar when detecting the forward and backward movements. The distance between the proximity sensor and the hand is another factor that can influence the magnitude of the output signal on the corresponding channel. It is used for a supplementary control.

The Virtual Joystick projects the hand movement in the 3D input space through the standard joystick interface and, when the function of tremor acquisition is used, this signal will be send through the standard serial line.

The paper is organized as following: in sections 2 and 3 the methodology, the reason of the specific acquiring mode and the extracted features, all related to the tremor signal, are presented. In section 4, we show that the new input device acquires and preserves all components from the tremor signal. In the next two sections, the method used to highlight the existence of different physiological and psychic fatigue states reflected in the tremor signal, the classifier system, and the performances obtained are presented. The last section concludes the paper.

## 2. The subjects and methods

### 2.1. The subjects

We admitted six (healthy people) subjects for this study. Two of them are women and the rest are male. Five of them are young people ( $26.6 \pm 3$  years, mean  $\pm$  standard deviation) and only one is 53-years old man. An informed consent was obtained from all the subjects.

### 2.2. The protocols

In a session of recording, each subject effectuated four recordings. Each subject carried out 90 seconds of tremor recordings followed by other subjects until all subjects completed four such recordings. In the last cycle, before the hand tremor acquisition, the subjects were required to hold in their hands an object (weighting about 4 Kg) until they were unable to keep it any more. In this way fatigue was induced. Per day two sessions of recordings were done. One session was made at 8<sup>00</sup> a.m. in the morning, when all the subjects were assumed to be rested, and the second was made at 14<sup>30</sup>, in the afternoon, when we considered that all the subjects were already tired.

In all this time, between these two sessions, the subjects were requested to do the usual daily activity. The recordings were made during a period of seven days. In all recording cycles the subjects were asked to maintain the same position of the hand above the bottom (bigger one) Virtual Joystick sensor. The initial position was with the hand placed parallel with the transducer and the center of the palm pointing exactly to the center of the transducer. All the users fixed the hand at the same vertical distance from the sensor, marked by a rule maintained in the position by a support. The subjects were seating.

Because fatigue is expected to influence the last part of the 90 seconds of the recording cycle, only the first 20 seconds and the last 20 seconds have been stored and analyzed. In all the time the subjects had no visual control of the hand position neither directly, nor through visual interface. In this mode, we prevented any possibility of biofeedback.

For the research described here, the sampling rate was 250 samples per second and we got 10.000 samples per each cycle of recordings: 5.000 corresponding to the first 20 seconds and the others corresponding to the last 20 seconds of recordings. Based on each of the 20 seconds segments, we extracted nine features. Two features vectors of nine features characterize a cycle for one subject. In a session, 48 points in a nine dimensional features space were collected (2 features vectors/cycle/user x 4 cycles x 6 users). Thus, in a day, 96 points and, respectively, at the end of seven days, 672 vectors of features were obtained.

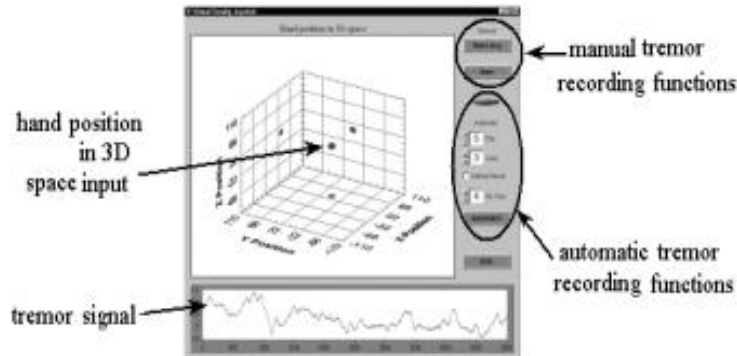


Fig. 2 – A view with the main window of the PC program, with the dot representing the hand sensed by the Virtual Joystick

The software used to manage the tremor acquisition and to store the data was written in Microsoft<sup>TM</sup> Visual C++ with the Measurement Studio ComponentWorks++ from the National Instruments<sup>TM</sup> and it is a improved version of the software presented in [8] and [9].

### 3. Signal processing

The signal-processing phase combines two stages: the pre-processing part, used to remove the main perturbation, and the feature extraction stage that was used to differentiate between the two physical states, rested and tired.

#### 3.1. Pre-processing

In our system the Virtual Joystick device low-pass pre-filtered the tremor signal at 60 Hz with an external, linear phase response, digital filter (a Bessel filter). Then, the signal was sampled with a frequency of 250 Hz and digitized on 12 bits. Fig. 3 presents one of these signals.

The tremor is a complex movement, composed by components derived from the respiratory movements and from other movements, unrelated with tremor like heart movements. The respiration, also, contributes at the low frequency spectrum of the hand tremor signal. These components must be removed, knowing that the respiration has a basic frequency around 0.1 up to 0.3 Hz for adult subject with a band in the range of 0.05 to maximum 3 Hz. After the PC software receives, in a serial mode, the tremor signal, Fig. 3(a), a high-pass filtering at 1 Hz is applied, Fig. 3(b). After smoothing the resulting signal, the software gets the signal shown in Fig. 3(c).

Using the moving average method with a window of 10 samples did the smoothing.

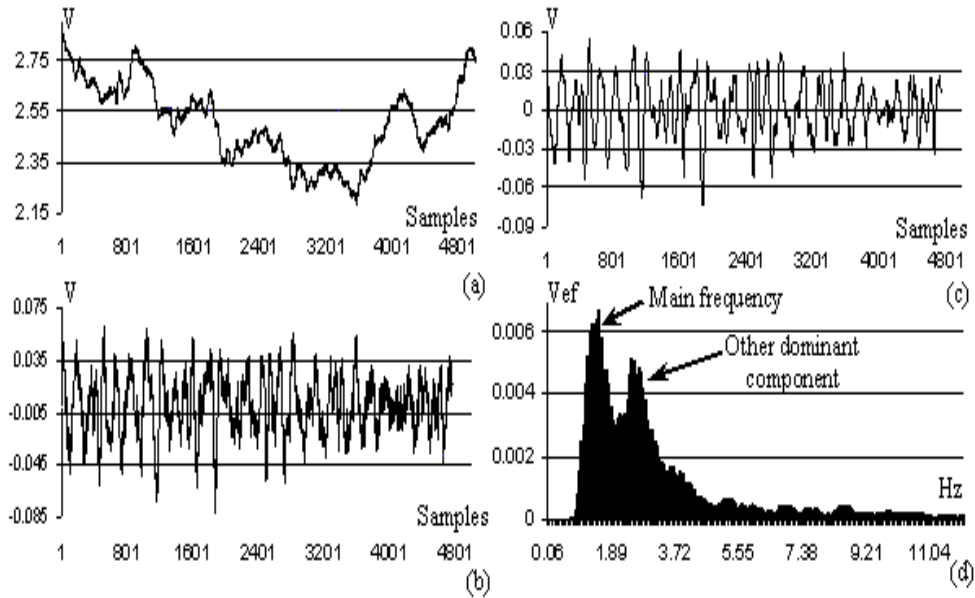


Fig. 3 – Example of tremor signal and some of the pre-processing steps

Mainly, because parts of the extracted parameters are in the frequency domain and because an accurate spectral measurement is wanted, a windowing technique was used to minimize the spectral leakage problem. The Hanning window was chosen based on its good frequency resolution (the width of the main lobe at  $-3\text{dB}$  is 1.44 bins) and base on it low spectral leakage (the side lobes roll-off rate is 60 dB/decade).

### 3.2. Choice of the features

Nine parameters are extracted from the tremor time series for each particular recording. These parameters are the main frequency, the frequency spreading, the width of the main frequency component, the variance of the width for the main frequency component, the power of the signal, the power variance, the high-frequency content to low frequency content ratio, named “high-to-low ratio”, the variance of the high-to-low ratio, and the signal standard deviation.

The “main frequency” component is defined as the frequency corresponding to the highest peak in the Fourier spectrum, Fig. 3(d). The “main frequency” of the tremor signal is an important parameter and most of the researchers use it [10], [11]. To estimate the actual “main frequency” and to overcome the picket-fence effect, we perform a weighted average of the frequency around maximum detected peak in the power spectrum. Namely we used:

$$f_{estimated\ main\ frequency} = \frac{\sum_{i=j-3}^{j+3} (Power(i) \cdot i \cdot \Delta f)}{\sum_{i=j-3}^{j+3} Power(i)} \quad (1)$$

where  $Power(i)$  is the power of the  $i^{th}$  bin,  $j$  the index of the highest detected pick, and  $\Delta f = f_s / N$  ( $f_s$  – the sampling rate,  $N$  – number of window points). In this case,  $f_s = 250$  Hz and  $N = 1024$  samples,  $\Delta f = 0.244$  Hz. A moving window of 1024 samples was used only for the algorithms that determine the “main frequency”, frequency spreading and the width of the main frequency component. Choice is justified by the reason to get a very good frequency resolution. For the other features, the window was of 512 samples. The choice of the span parameter in the range  $\pm 3$  is suitable for two reasons. First, because it represents a spread wider than the main lobe of the Hanning window and second, from the point of view of the tremor signal, it is wide enough and, also, the possibility of interfering with a possible second main frequency component is lower.

The width of the main frequency component was estimated with the relation:

$$\Delta f_{width} = \frac{\sum_{i=j-3}^{j+3} Power(i)}{7 \cdot NPBW \cdot Power(j)} \quad (2)$$

where  $NPBW$  is the noise power bandwidth of the window.

We have confirmed the remark [12], observed in several cases, that under muscular effort the tremor signal spectrum starts to change significantly (the main frequency decreases and the movement becomes more regular with lower contents in higher frequency).

Based on these facts, another parameter was chosen in order to discriminate between the rested and the tired state. This parameter is the ratio between the low frequency region and the high frequency region energy in the spectrum, using the threshold of 6 Hz. This boundary frequency is assumed to exist between the “low-frequency tremor” and the “high-frequency tremor” [13].

Physicians fixed this boundary parameter starting from a pathological point of view related with the tremor signals. In our case, with all the subjects in a healthy condition, after the visualization of the spectral components, we determined that the power of the signals concentrated around the lower part of the spectrum and only a small quantity is past the 6 Hz boundary.

Therefore, we tested the hypothesis that the 4 Hz boundary, used in the previously defined parameter, is more appropriate for ours objectives or it is not.

#### 4. The ability of the sensor to acquire tremor signals

From the beginning, one of the main requirements imposed to the Virtual Joystick design was its ability to acquire a tremor signal and simultaneously the hand movement. This should happen without any compromise in the hand tracking mechanism and in the quality of the tremor signal. The tremor signal must be a very reliable one. It must preserve all non-linear stochastic or chaotic components that a classification system can take advantage from. Previous researches [12], [14] indicate that tremor includes a significant nonlinear, chaotic component, but stochastic components are also expected [12], [14], [15].

The objectives mentioned above was achieved by using a set of techniques (soft and hard) and technologies dedicated to this goal [8] as following:

- the bandwidth of the transducer is appropriate for the acquisition of the tremor signal [5]; basically, this is due to the high frequency operation of the sensors;
- the mode of setting the work of the sensor in the linearity part of the sensor characteristic;
- the processing techniques involved in the tremor path of the signal, like filters with linear phase characteristic;
- the precaution used to acquire the tremor signal, the sampling rate, the number of bits used by the converter (12 bits) – mainly because the sampling and quantization noise can generate unreliable results, destroying the noise sensitive nonlinear information in the tremor signal;
- the software solution used in the subroutine implied in the data transfer between the multimodal virtual joystick and the PC (the serial transfer between the joystick and the personal computer take a lot of time. For this reason, a different thread of program execution was dedicated to the tremor signal transfer and, in this mode, we had no interference between the hand tracking part of the system and the tremor transfer).

In [10], the nonlinear analysis was performed with the help of the correlation dimension and the Lyapunov exponent. The values of the Lyapunov exponent started with almost 0 (0.05) and went up to 0.7; the correlation dimension of the tremor signal was in the range of 0.5 up to 5, but many of the recordings exhibited a correlation dimension value in the range 2.5 to 3.

To determine the correlation dimension and the Lyapunov exponent, we first need to establish the embedding dimension value for the state space reconstruction. For this, the mutual information function [16] was used to determine the optimal value of the time delay parameter. The obtained time delay parameter was around 33 for most of the tremor series, like in Fig. 4(a). The minimum embedding dimension was, then, calculated for a one-dimensional time tremor series by using the time delay information as the input parameter for the *False Nearest Neighbors* method.

In Fig. 4(b), we are present the results for one tremor time series, randomly chosen for our analysis.

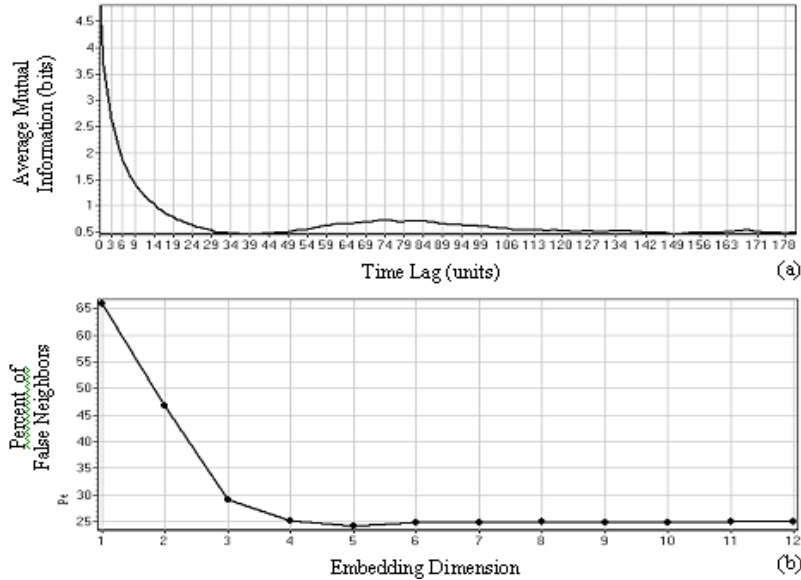


Fig. 4 – (a) average mutual information and (b) embedding dimension for a time series

The resulting minimum percent of false neighbors was reached somewhere around the embedded dimension of 5. For almost all time series, the embedding dimension resides in the range from 5 to 9. But, for a few number of time series the embedding dimension is equal with 10. All of the above determinations were completed with the Visual Recurrence Analysis [17] program, version 4.2.

First, the correlation dimension (CD) was calculated in order to get an image about the level of “complexity” of the associated time series. The correlation dimension of the processed tremor signal was in the range 2.572 to 4.407. In all analysis performed the tremor signal was high pass filtered at 1 Hz and smoothed with a moving window of 10 samples. The chaotic character of the time tremor series was tested using Lyapunov exponents. The values found for the Lyapunov exponent were in the range [0.04, 0.18]. This range shows the presence of a “light” chaotic behavior.

## 5. The fatigue state analysis

The number of clusters for the data set can be determined: (1) a priori, (2) automatically, by using a cluster validity measure [18], (3) by an iterative process of inserting a new cluster center in the algorithm [19] until a validity measure begins to decrease, or by a method of combining the already existing clusters. In this paper, an iterative process was used to determine the correct number of clusters. In spite that the problem we tried to solve seems to be a quite simple one – we may assume to have two classes (rested and tired subjects) – the problem is not



that simple. The first attempts to directly classify the features vectors extracted from the tremor signal in two classes gave poor results. From the starting point, in the recording methodology, we took into consideration several distinct situations. In the data sets acquired in the morning at least two different categories it can be distinguished: the recordings effectuated after the subjects were asked to keep in their hand a heavy load (thus, fatigue was induced by force), and second, the other recordings.

In a similar way, we can distinguish between two categories in the recordings obtained during the afternoon. Several questions may arise. Does there exist any difference between the fatigue induced in the morning by short periods of intense muscular activity and the *neuro-muscular* fatigue state attained in the afternoon? Is it possible that the first one to be pure physiological fatigue while the second one to be a combination between physiological and neuro-muscular or psychological fatigue state? Is it possible to make a difference between these two fatigue states, supposed different? To answer the above questions, we used a k-means clustering algorithm on two different sets of data, used to discriminate between some of the cases previously presented.

To get an idea of how well separated are the clusters, a silhouette parameter was calculated for every features vector. The silhouette parameter represents a measure of how similar is a point with the points from the right cluster compared with the points from the other clusters. The value of the silhouette parameter is in the range -1 to 1. If the silhouette takes the value 1, the object is well classified and it is very distant from the neighboring clusters. A zero value symbolizes points that are not distinctly in one cluster or another; and, in the mean time, a value of -1 means that the point was badly classified. Let us suppose that we have found a clustering of the objects into  $k$  groups;  $A$  is the cluster to which the features vector  $x_i$  belongs to, and  $C_k$  represents any cluster different from  $A$ . Then, the silhouette parameter is defined as:

$$\text{silhouette}(x_i) = \frac{b(x_i) - a(x_i)}{\max[a(x_i), b(x_i)]} \quad (3)$$

where

$$a(x_i) = \frac{1}{\text{no}\{A\} - 1} \sum_{j \in A, j \neq i} d(x_i, x_j) \quad (4)$$

$$b(x_i) = \min_{C_k \neq A} \{d(x_i, C_k)\} \quad (5)$$

$$d(x_i, C_k) = \frac{1}{\text{no}\{C_k\}} \sum_{x_j \in C_k} d(x_i, x_j) \quad (6)$$

and  $d(x_i, x_j)$  represents the distance between  $x_i$  and  $x_j$  features vector;  $no\{A\}$  is the number of elements that compose the cluster  $A$ .

In [20] it was proposed, for the first time, the idea of using the mean silhouette parameter in order to assess, determine and estimate the optimal number of the clusters. The method chooses the optimal number of clusters, which is the number of clusters that maximize the average silhouette value over the entire data set. The experience has led us to the subjective interpretation of the silhouette coefficient as listed in table 1.

Because the k-means algorithm faces several problems (like sensitivity to noise data and outliers, the cluster must to have a convex shape, the cluster algorithm often terminates in a local minimum) a number of precautions must be taken. All the results presented bellow were chosen by selecting the best one from a sets of several results obtained from the ten repeated instance of the clustering algorithm, each with a new set of initial clusters centroid position. In this way, we tried to overcome the possibility to be captive in a local optimum.

To eliminate the outlier problem, we worked with two different data sets. In the first one, all the particular data segment sets were eliminated if at least one feature was outside the range  $[-3\sigma, +3\sigma]$ , where  $\sigma$  represents the spreading of the particular feature. In the second one, the range was reduced to  $[-2\sigma, +2\sigma]$ .

The results presented below are obtained using the first set; this is mostly because no significant results were observed with the reduced data sets and, more, because we need, in the second step (when we classify the data) to have a large training set.

Table 1

Interpretation of the silhouette coefficient

Silhouette value	Interpretation
0.71 ... 1.00	Strong structures have been found.
0.51 ... 0.70	Reasonable structures have been.
0.26 ... 0.50	The structures are weak and could be artificial try another methods.
< 0.25	No substantial structure has been found.

In the first test, only the data set acquired in the morning was used. In this way we want to see if there exist a difference between the fatigue-state induced by force and the normal, resting state. The clustering algorithm was started, for the beginning, with two clusters. After the iterative process – consisting in features vectors reassignments and clusters centers re-calculating – was finished, the plot for the silhouette parameters for the entire data set was computed and presented in Fig. 5(a). These results were obtained using the 6Hz boundary for the ratio between the low frequency region and the high frequency region power parameter in the features vector.

The mean value of the silhouette parameter was 0.3905 for the case with two classes. When we increased the number of the clusters, the average silhouette took

the value of 0.3539 for the particular case with three classes; when we further increased the number of clusters, the average silhouette decreased continuously. We conclude that the correct number of clusters is two, this highlighting the possibility to differentiate between the two cases presented.

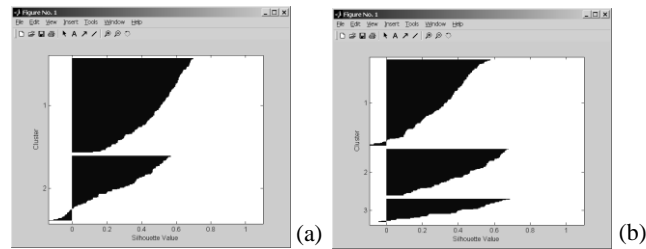


Fig. 5 – The silhouette plot for (a) two classes, (b) three classes - for all recordings acquired in the morning.

In order to appropriately estimate the frequency boundary value for the high to low ratio parameter, the k-means clustering algorithm was restarted with a new set of features vectors, using this time the 4 Hz boundary value and preserving the other condition previously presented. The mean value for the silhouette parameter was 0.3904 in the case of two classes and 0.3536 for three classes and continued to decrease when we increased the number of classes. These observations suggest that no important improvements can be reached when 4 Hz boundary was used.

In the second test, we tested the possibility to differentiate between the fatigue state induced by force and the fatigue state that is occurring normally at the end of the workday. To differentiate between the two fatigue states, the training set was composed only by the recordings acquired in the morning, in the condition of fatigue state induced by force, and by the entire set recorded in the afternoon. The average silhouette value for the two classes was 0.4074 and it went up to 0.4565 for the case of three classes; after that, it started to decrease with the increasing number of the classes. For example, for three classes the mean silhouette value took the value of 0.374. The boundary for high-to-low ratio parameter was 6 Hz.

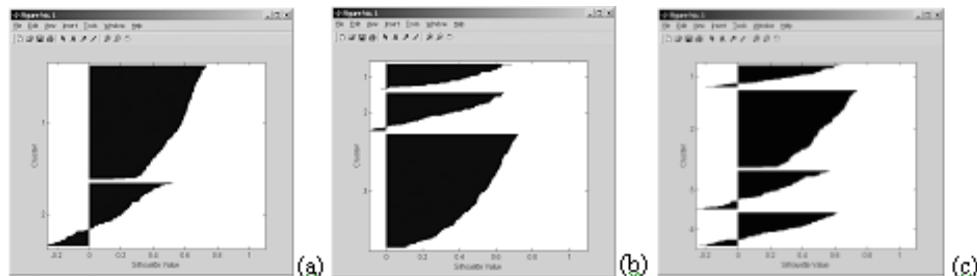


Fig. 6 – The silhouette plot for (a) two, (b) three and (c) four classes; using the 6 Hz boundary for high-to-low ratio parameter.

When the boundary was set at 4 Hz, the mean silhouette value, according to Fig. 7, took the 0.4074 value for two classes, 0.4566 for three classes and 0.3738 for four classes. Once again we do not observe any significant improvement.

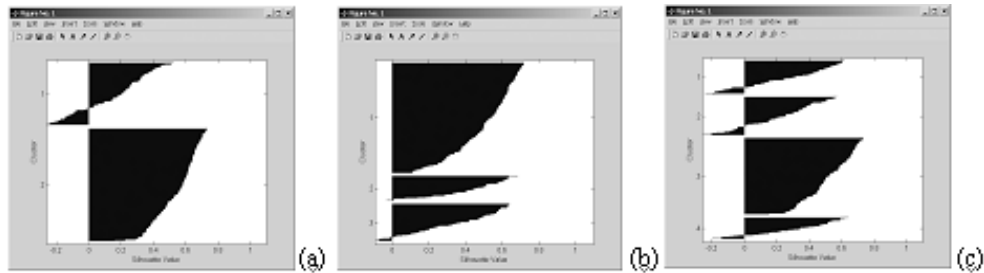


Fig. 7 – The silhouette plot for (a) two, (b) three and (c) four classes; using the 4 Hz boundary for high-to-low ratio parameter.

We found of interest the ability to differentiate not only between the fatigue state induced by force (mainly muscular fatigue) and the fatigue state normally installed at the end of the workday, but more – in the data sets recorded in the afternoon, we can differentiate between the two particular fatigue states. Notice that, in table 1, for our range of mean silhouette values, one of the possible interpretation is that the structures observed could be artificial and, in conclusion, the entire analysis presented above could be false. But, because we know the labels of the features vectors and based on the results presented in the next section, we concluded that the hypotheses of weak data structures is the correct one.

Weights of hebbianFull									
	0	1	2	3	4	5	6	7	8
0	0.729209	0.000017	0.000030	0.000023	0.000104	0.000004	0.000054	0.000185	-0.000144
1	0.000017	0.364246	-0.000043	-0.000019	0.000015	0.000074	-0.000152	-0.000073	-0.000063
2	0.000030	-0.000043	0.198803	-0.000007	-0.000002	-0.000002	0.000022	-0.000037	0.000130
3	0.000023	-0.000019	-0.000007	0.118694	-0.000002	0.000005	0.000006	-0.000009	-0.000142
4	0.000104	0.000015	-0.000002	-0.000002	0.097688	0.000001	0.000012	-0.000005	0.000241
5	0.000004	0.000074	-0.000002	0.000005	0.000001	0.068099	-0.000006	0.000011	0.000459
6	0.000054	-0.000152	0.000022	0.000006	0.000012	-0.000006	0.025435	0.000104	0.001064
7	0.000185	-0.000073	-0.000037	-0.000009	-0.000005	0.000011	0.000104	0.022828	-0.002937
8	-0.000144	-0.000063	0.000130	-0.000142	0.000241	0.000459	0.001064	-0.002937	0.000795

Fig. 8 – The diagonal covariance matrix for the output of the PCA network; where on the diagonal are the eigenvalues

## 6. Classification of the subject state

In order to develop a deeper understanding of the features space complexity, we used PCA to visualize if there exist clear structures in the new set of data (principal components data) obtained at the output of the PCA networks. The analysis was done for all data sets and for all subjects. In the next part of the PCA analysis, the results are presented only for one subject data set. We used for the

visualization only the first six outputs of the PCA network. These outputs represent 96.983 % of the power of all the features involved. In Fig. 8, we present the weights of the forced Hebbian network. The Hebbian network was used to compute the covariance matrix of the PCA outputs data sets. The diagonal elements of the covariance matrix are the eigenvalues of the PCA output data sets.

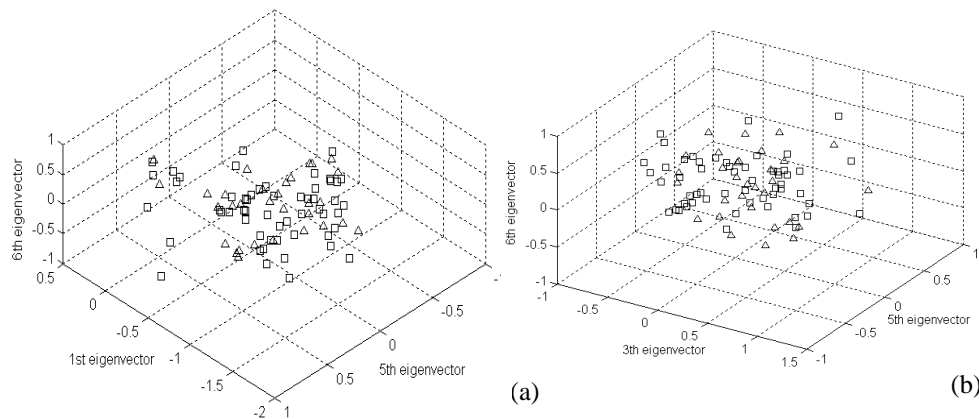


Fig. 9 – Two distribution of the user state (rest-triangle/tired-square) on the (a) first, fifth and sixth eigenvector axes space and (b) third, fifth and sixth eigenvector axes space

In spite of the fact that in the projected eigenvector space the data cluster in some parts of the space, Fig. 9(a) and (b), the overall impression is that the data from both classes are scattered and mixed in all the space and no clear clusters can be found. This conclusion was derived after several visualizations, made for different angles of the 3D space and for all possible combinations of the first six eigenvectors. For this reason, a Support Vector Machines was chosen for the classification part; its main idea is that in a high dimensional space, the data become linearly separable.

The Support Vector Machine (SVM) was implemented in NeuroSolution (a demo version), by using the kernel Adatron algorithm [21]. The kernel Adatron algorithm is an on-line version of the Vapnik's original algorithm and it is effective in separating sets of data, which share complex boundaries, like in our case. After a map into a high-dimensional feature space is accomplished, the algorithm optimally separates data into their respective classes by isolating those inputs that fall close to the data boundaries in order to maximize the output perceptron margins. The two classes described by the support vector machine classifier can be expanded to a N-classes classifier (in our situation  $N = 4$ ). This could be done by constructing N classifiers each one classifying two classes ( $\{\text{class } i\}$  versus  $\{\text{class } 1 \dots N / \text{except } i\}$ ) and, then, determining the correct class (choose the class that yields the maximum value among the all N classifiers).

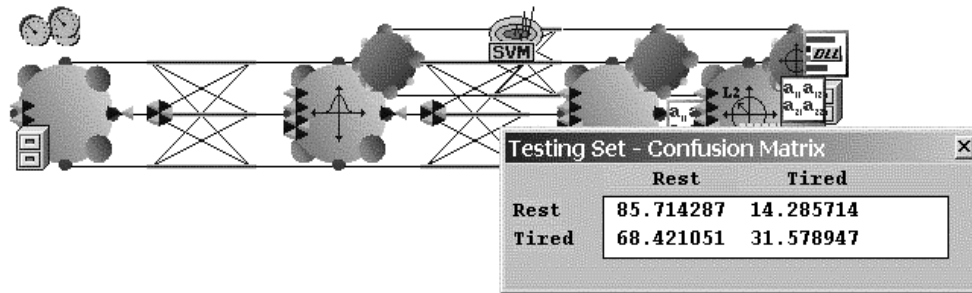


Fig. 10 – The support vector machine network implemented in the NeuroSolution environment and the performance obtained on a test set

Table 2

The confusion matrix for the experiment results

	Rested	Fatigue
Rested	<b>85.71 %</b>	<b>14.29 %</b>
Fatigue	<b>68.42 %</b>	<b>31.58 %</b>

In Fig. 10, we exemplify with the network that classifies the rested and the tired states. The rested state is represented by all the recordings acquired in the morning but without the recordings' parts where the fatigue was induced by force (the recordings made after the subjects were asked to keep in their hand a heavy load); the rest of the recordings represents the tired state. The performance of the classifier is shown in table 2. Although these results are preliminary, we observe good performance of 31.57 % correct status recognition in the case of tired state and 85.71 % for the rested state. Because we are interested only in discovering the tired subjects, this preliminary result is promising. These results are good, because we identify the tired state only from the tremor signal and do not use other type of information.

The results for the cases when we tried to discriminate between the fatigue states – induced by force in the morning or in the afternoon – and the other states were very weak. This happens because both training sets are not statistical representative. If we consider only the case of the fatigue induced by force in the morning, this data set represent 11.86 % (69 features vectors) from the entire data set. Moreover, if we take into account the cross validation and the test sets extracted from the same original data set, we can get a clear image regarding the poor results.

When we used the high-to-low ratio parameter with the 4 Hz boundary in the Support Vector Machine classification algorithm no important improvements were observed. Based on this observation and from the ones presented above we can conclude that the 4 Hz frequency boundary do not offer superior performances.

## 7. Conclusions

Tremor assessment in medical investigation is not a well-developed technique yet. Apart the assessment of Parkinsonian tremor, the mechanics of tremor generation in normal subjects and in several conditions like diseases, intoxication, and age-related conditions is not well understood. Tremor in normal subjects has been known for a long time to be related to emotion and fatigue, but the mechanisms producing these tremor movements and the specific characteristics of such tremor movements are not well known.

Tremor signal analysis is not a simple task, from the engineering point of view. Apart the acquisition problem, requiring non-contact transducers able to pick-up the movements of different parts of the hand, the superposition of various types of non-tremor movements asks for a signal separation technique. Classification of tremor movements is somewhat blind, because little is known on the classes, from the medical point of view. But, as we can see from the reported results, in the tremor signal it exists significant information related to the subject's state. But, more must be done in this direction in order to obtain a reliable decision system.

In this research, we presented several new results related to analyzing, classifying, and assessing tremor movements, in view of applications in man-machine intelligent interfaces and in medicine.

## Acknowledgements

This work was partially supported by Romanian National Council for Research in High Education Grant 75/2003 and by IEEE NNS Walter Karplus Summer Research Grant. The sensor is protected by a patent [5] and any attempt to use the sensor without written permission of Horia-Nicolai Teodorescu and the owners of the patents is forbidden. This paper does not create any rights for use of the sensor described herein and in [5] by any person or institution.

## References

- [1] W. ARK, D. DRYER, D. LU: *The Emotion Mouse*, Proceedings of 8th International Conference on Human-Computer Interaction, Vol. 1, New Jersey, SUA, pp. 818-823, 1999
- [2] V. CORNELLIER, T.K. ZIEGLER: *Biomonitoring stress management method and device*, Patent No. 4,683,891, United States, Publication date: 1987, August 4<sup>th</sup>
- [3] E. VYZAS, R. W. PICARD: *Affective Pattern Classification*, Proceedings of the AAAI Fall Symposium Series: Emotional and Intelligent: The Tangled Knot of Cognition, Orlando, Florida, United States, 1998.
- [4] FREDERIC DE COULON, E. FORTE, D. MLYNEK, H.N. TEODORESCU, S. SUCEVEANU: *Subject-State Analysis by Computer and Applications in CAE*, Proceedings of the International Conference on Intelligent Technologies in Human-Related Sciences, July 5-7, 1996, Leon, Spain, pp. 243-250, 1996.
- [5] H.N. TEODORESCU: *Position and movement resonant sensor*, Patent No. 5,986,549, United States, Publication date: 1999, October 14.

- 
- [6] H.N. TEODORESCU, D.M. DOBREA, E. FORTE, M. WENTLAND-FORTE: *A High Sensitivity Sensor for Proximity Measurements and Its Use in Virtual Reality Applications*, Proceedings of the European Conference on Intelligent Technologies, ECIT'2000 International Conference, Romania, Iasi, 2000.
- [7] D.M. DOBREA, H.N. TEODORESCU, D. MLYNEK: *An Interface for Virtual Reality Applications*, Romanian Journal of Information Science and Technology, Vol. 5, No. 3, pp. 269 – 282, 2002.
- [8] D.M. DOBREA: *A New Type of Non-Contact 3D Multimodal Interface to Track and Acquire Hand Position and Tremor Signal*, Proceedings of European Conference on Intelligent Technologies, July 20-22, Iasi, Romania, 2002.
- [9] D.M. DOBREA, H.N. TEODORESCU: *A Fuzzy System Used to Derive Hand Movements from a New Virtual Joystick Interface Device*, Scientific Bulletin of The "POLITEHNICA" University of Timisoara, Vol. 1, No. 47, pp. 27 – 31, 2002.
- [10] H.N. TEODORESCU, M. CHELARU, A. KANDEL, I. TOFAN, M. IRIMIA: *Fuzzy methods in tremor assessment, prediction, and rehabilitation*, Artificial Life in Medicine, Vol. 21, pp. 107-130, 2001.
- [11] J. TIMMER, M. LAUK, W. PFLEGER, G. DEUSCHL: *Cross-spectral analysis of physiological tremor and muscle activity. I: Theory and application to unsynchronized EMG*, Biological Cybernetics, Vol. 78, pp. 349-357, 1998.
- [12] H.N. TEODORESCU, A. KANDEL: *Nonlinear Analysis of Tremor and Applications*, Japanese Journal of Medicine Electronic Biomedical, Vol. 13, No. 5, pp. 11-20, 1999.
- [13] A.W. ANOUTI, C. KOLLER: *Tremor disorders. Diagnosis and management*, West J. Med, Vol. 162, No. 6, pp. 510-513, 1995.
- [14] J. TIMMER, S. HÄUSSLER, M. LAUK, C.H. LÜCKING: *Pathological tremors: Deterministic chaos or nonlinear stochastic oscillators?*, Chaos, vol. 10, no. 1, pp. 278-288, 2000.
- [15] S. LOZNEANU, H.N. TEODORESCU: *Models for temporal patterns generation in stochastic cellular systems*, Proceedings of the 9th Int. EMBS Conference IEEE, vol. 3, Boston, United States, pp. 1461-1462, 1987.
- [16] A.M. FRASER, H.L. SWINNEY: *Independent coordinates for strange attractors from mutual information*, Physics Review A, vol. 33, no. 2, pp. 1134-1140, 1986.
- [17] The official WEB page for the software product Visual Recurrence Analysis is: <http://pw1.netcom.com/~eugenek/download.html>
- [18] N.R. PAL, J.C. BEZDEK: *On cluster validity for the fuzzy c-means model*, IEEE Transaction on Fuzzy Systems, vol. 3, no. 3, pp. 370-379, 1995.
- [19] I. GATH, B. GENEVA: *Unsupervised Optimal Fuzzy Clustering*, IEEE Transaction on Pattern Analysis And Machine Intelligence, vol. 11, no. 7, pp. 773-781, 1989.
- [20] L. KAUFMAN, P. ROUSSEEUW: *Finding Groups in Data: An Introduction to Cluster Analysis*, John Wiley & Sons Inc., New York, 1990.
- [21] J.C. PRINCIPE, N.R. EULIANO, W.C. LEFEBVRE: *Neural and Adaptive Systems: Fundamentals Through Simulations*, ed. John Wiley & Sons Inc., New York, 2000.